Multiresolution Time Domain Modeling for Large Scale Wireless Communication Problems

Costas D. Sarris[1], Karen Tomko[2], Pawel Czarnul[3], Shih-Hao Hung[3], Robert L. Robertson[1], Donghoon Chun[1], Edward S. Davidson[3] and Linda P. B. Katehi[1]

[1] Radiation Laboratory, EECS, University of Michigan, Ann Arbor

[2] Department of Electrical and Computer Engineering and Computer Science, University of Cincinnati

[3] Advanced Computer Architecture Laboratory, EECS, University of Michigan, Ann Arbor

Abstract

The time domain modeling of large scale cosite interference problems, arising in wireless communication channel analysis and design studies, is discussed in this paper. It is pointed out that the use of the conventional Finite Difference Time Domain method for the treatment of such problems typically results in long, computationally burdensome simulations that limit the ability of this technique to provide an efficient CAD - oriented tool for commercial and military applications. For the purpose of accelerating these simulations, the use of wavelet based time domain solvers along with parallelization techniques is proposed.

I. Introduction

With the recent advances in mobile communications and their growing use in commercial and military applications, the rigorous analysis of electromagnetic intereference (EMI) between antennas mounted on neighboring platforms has become a topic of critical importance. In particular, the concurrent operation of tranceiver systems in proximity with each other and their resultant parasitic reception of interfering signals, can potentially drive their power amplifier stages to saturation, causing the well - known effect of desensitization that can even block the operation of radio networks [1]. For the complete theoretical characterization of desensitization and the physical understanding of its phenomenology, the integrated modeling of both electromagnetic wave propagation across a given channel and the wave interaction with tranceiver front-end electronics is motivated.

For this dual purpose, time domain techniques such as the Finite Difference Time Domain (FDTD) are well suited as they offer a mathematically straightforward and inherently versatile method for the analysis of arbitrary electromagnetic geometries. Furthermore, it was recently demonstrated that the incorporation of active element components and nonlinear circuits in the FDTD mesh can be easily accomplished by following a state equation based approach [2]. However, as FDTD is a second order accurate scheme, and sensitive to numerical dispersion, a dense discretization of at least ten, but usually twenty five points per wavelength is necessary for the extraction of a convergent solution. Hence, the FDTD treatment of electrically large domains corresponding to geometries of cosite vehicular tranceivers (even in VHF band operation), yields a computationally intensive, memory and execution time consuming calculation.

For the alleviation of the computational burden involved in FDTD simulations, this paper follows two directions of research. The first is the use of parallelization for the distributed update of the electromagnetic field values in the computational domain over several processors, while the second is the introduction of wavelets for the implementation of a space and time adaptive gridding via the Multiresolution Time Domain (MRTD) technique [3], in the sense of [4]. The Haar wavelet basis is employed, for the reason that its update equations include only nearest neighbor interactions, in contrast with higher order basis functions, whose stencil extends over several cells. Thus, the Haar basis is considered as a promising candidate for the application of parallel computing to MRTD.

In the following, the aforementioned modeling approach is explained in greater detail and numerical results regarding typical problems that this work aims to address are provided.

II. The Three Dimensional Haar MRTD Scheme

The three dimensional Haar wavelet based MRTD scheme is formulated in this section. For this purpose, all electric and magnetic field components are expanded in three dimensional Haar scaling and wavelet functions ϕ, $\psi_{r,p}$ with $r = 0, 1 \cdots r_{max}$ being an index denoting the resolution of the wavelet term (varying from 0 to r_{max}) and $p(r) = 0, 1, \cdots 2^r - 1$ being a counter of the r-order wavelets within each cell. The mathematical definition of the Haar scaling and wavelet functions is given in [5]. It is noted that the introduction of one wavelet level (zero order) in x, y, z is expected to bring about an improvement in resolution of a factor of two per direction (hence, eight in total) compared to a scaling only based scheme. However, for this to be true, a certain condition regarding the arrangement of electric and magnetic field nodes need be imposed, as discussed in [6]. Namely, as the offset of electric and magnetic field nodes is half a cell in FDTD, in an $r-$order Haar MRTD (of $r+1$ - wavelet levels) this offset must be

Research supported by the Army Research Office under the project for "Efficient Numerical Solutions to Large Scale Tactical Communication Problems" (DAAD19-00-1-0173).

0-7803-7070-8/01/$10.00 ©2001 IEEE

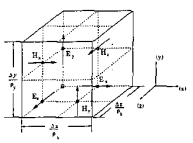

Fig. 1. Equivalent Yee's cell for Haar MRTD.

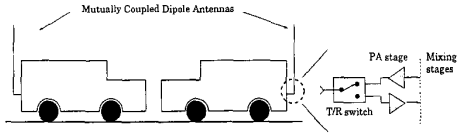

Fig. 2. Cosite interference scenario including dipole antennas mounted on two neighboring vehicles.

set equal to one cell by 2^{r+2}. For example, the E_x component of the electric field is expanded as :

$$
\begin{aligned}
E_x(\bar{r},t) \;=\; & \sum_{n} h_n(t) \sum_{i,j,k} \left\{ {}_nE^{\phi\,\phi\,\phi}_{i',j,k}\phi_{i'}(x)\phi_j(y)\phi_k(z) + \sum_{r_z,p_z} {}_nE^{\phi\,\phi\,\psi_{r_z,p_z}}_{i',j,k}\phi_{i'}(x)\phi_j(y)\psi^{r_z}_{k,p_z}(z) \right. \\
& + \sum_{r_y,p_y} \left\{ {}_nE^{\phi\,\psi_{r_y,p_y}\,\phi}_{i',j,k}\phi_{i'}(x)\psi^{r_y}_{j,p_y}(y)\phi_k(z) + \sum_{r_z,p_z} {}_nE^{\phi\,\psi_{r_y,p_y}\,\psi_{r_z,p_z}}_{i',j,k}\phi_{i'}(x)\psi^{r_y}_{j,p_y}(y)\psi^{r_z}_{k,p_z}(z) \right\} \\
& + \sum_{r_x,p_x} \left\{ {}_nE^{\psi_{r_x,p_x}\,\phi\,\phi}_{i',j,k}\psi^{r_x}_{i',p_x}(x)\phi_j(y)\phi_k(z) + \sum_{r_z,p_z} {}_nE^{\psi_{r_x,p_x}\,\phi\,\psi_{r_z,p_z}}_{i',j,k}\psi^{r_x}_{i',p_x}(x)\phi_j(y)\psi^{r_z}_{k,p_z}(z) \right\} \\
& \left. + \sum_{r_x,p_x,r_y,p_y} \left\{ {}_nE^{\psi_{r_x,p_x}\,\psi_{r_y,p_y}\,\phi}_{i',j,k}\psi^{r_x}_{i',p_x}(x)\psi^{r_y}_{j,p_y}(y)\phi_k(z) + \sum_{r_z,p_z} {}_nE^{\psi_{r_x,p_x}\,\psi_{r_y,p_y}\,\psi_{r_z,p_z}}_{i',j,k}\psi^{r_x}_{i',p_x}(x)\psi^{r_y}_{j,p_y}(y)\psi^{r_z}_{k,p_z}(z) \right\} \right\}
\end{aligned}
\tag{1}
$$

where $i' \equiv i + 1/2^{r_{x,max}+2}$, $r_{x,max}$ denotes the maximum wavelet order in $x-$direction and h_n are the pulse functions defined in [3]. The rest of the EM field components are accordingly defined. The combination of scaling and wavelet terms yields equivalent grid points whose arrangement (under the condition followed here) in the equivalent Yee's cell of MRTD is shown in Fig. 1, where $\rho_\xi = 2^{r_{\xi,max}+1}$, $\xi = x,y,z$ (refinement factor). Finally, a dispersion analysis of this scheme shows that its dispersion characteristics are given by the expression :

$$
\left\{\frac{1}{u_p\Delta t}\sin\frac{\omega\Delta t}{2}\right\}^2 = \left\{\frac{1}{\Delta x_{eff}}\sin\frac{k_x\,\Delta x_{eff}}{2}\right\}^2 + \left\{\frac{1}{\Delta y_{eff}}\sin\frac{k_y\,\Delta y_{eff}}{2}\right\}^2 + \left\{\frac{1}{\Delta z_{eff}}\sin\frac{k_z\,\Delta z_{eff}}{2}\right\}^2 \tag{2}
$$

where $\Delta x_{eff} = \Delta x/2^{r_{x,max}+1}$, $\Delta y_{eff} = \Delta y/2^{r_{y,max}+1}$, $\Delta z_{eff} = \Delta z/2^{r_{z,max}+1}$ and Δx, Δy, Δz are the scaling cell sizes. Equation (2) shows that unlike previous formulations of Haar MRTD that lacked the theoretically expected resolution properties [7], the scheme that is presented here does demonstrate an accuracy consistent behavior. The rest of our derivation follows the Method of Moments based technique that is set forth in [3].

III. Cosite Interference Problem Modeling

A. Geometry / Open boundaries

The general form of cosite interference scenarios considered in this work, is shown in Fig. 2 which depicts two neighboring vehicular tranceivers. Cases of more vehicular tranceivers or multiple antennas mounted on the same platform are also considered. For the simulation of the open boundaries of the domain, a uniaxial PML absorber [8] is employed, for both FDTD and MRTD simulations. In particular, MRTD mesh truncation via an FDTD UPML is used by means of an FDTD/MRTD interface, that provides for a stable transition from the one engine to the other with no need for interpolations or extrapolations in either space or time [9]. The condition for the stable/dispersionless matching of the two schemes, as given by Equation (2), is that the FDTD cell sizes be equal to the MRTD *effective* cell sizes. In our simulations, a separation of one to two wavelengths between the vehicles and a ten cell absorber of nominal reflection coefficient $\exp(-16)$ has been sufficient for the extraction of accurate results.

B. Active Elements

The assesment of the effect of cosite interference on the operation of the tranceiver front-end electronic equipment and especially input stage amplifiers is also of interest here. For this purpose, the "extended" FDTD method of [2] has been utilized. According to the method, circuit state equations (the circuit being the load at the antenna input port) are coupled with a Thevenin/Norton equivalent of the FDTD cell (derived by Maxwell's curl equations) in order to represent the circuit/ wave interaction. This technique has been successfully incorporated in MRTD simulations [10], due to its versatile, circuit theory based character.

C. Parallelization

The parallel FDTD algorithm currently uses a static regular block based partitioning strategy in which each processor is assigned one block of the domain to work on. The computational workload is non-uniform across the domain with little or no computation performed for cells within a vehicle and additional computations for cells within the absorber regions. The partitioning strategy uses relative computational weights for each type of cell to adjust the subdomain boundaries and compensate for this imbalance. The MPI library is used for communication between processors owning neighboring cells.

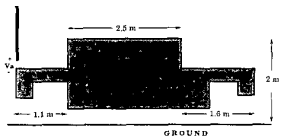

Fig. 3. Vehicle model.

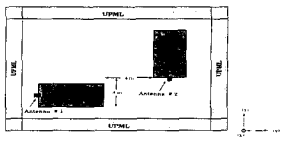

Fig. 4. Computational domain for the first cosite interference scenario ($yz-$ plane).

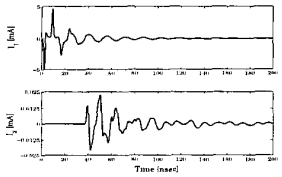

Fig. 5. Input currents for the two antennas of Fig. 4.

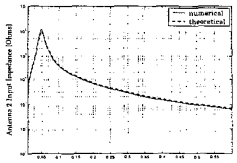

Fig. 6. Numerical and theoretical value of the input impedance of antenna 2 (Fig.4).

IV. Numerical Results

The vehicle model that is used in our simulations is shown in Fig. 3. The vehicle trunk is considered as a perfect electric conductor, an assumption that is valid in the VHF band. The vehicle antenna is modeled as a monopole mounted on the rear part of the platform. Two case studies are presented here, both including two neighboring vehicular tranceivers in hybrid operation (the one is in transmit and the other in receive mode). This operation is simulated by using a transparent, 0-0.6 GHz Gaussian excitation at the gap of the first antenna. For the derivation of the following results, the FDTD method is employed in both a serial and parallel fashion, with Yee's cell dimensions being equal to 5 cm by 5 cm by 5 cm. The receiving antenna is terminated at a parallel RLC block with $R = 1\ K\Omega$, $L = 1\ \mu H$, $C = 10\ pF$, that is modeled by means of the state equation approach of [2]. It is noted that the antennas are $x-$ directed and considered as one cell thick and one meter long. Local subgridding techniques can be readily employed for the modeling of thinner monopoles. Finally, the time step is equal to 92 $psec$. For the execution of parallel runs, the NPACI Blue Horizon teraflop-scale Power3 based clustered SMP system is used. The system has 1152 processors, 512GB memory which are arranged as 144 SMP nodes each with 8 375MHz Power3 processors and 4GB memory shared among them. Timing measurements correspond to 100 time-step runs, each being executed 3 times. Both average and minimum times are shown.

The first geometry under study is depicted in Fig. 4 and yields a relatively large working volume of 70 by 274 by 204 cells terminated into 10 UPML cells at each open boundary. Input current waveforms for the two antennas (derived by means of Ampere's law) are shown in Fig. 5. Even the apparently weak coupling between the two antennas can adversely affect the receive operation of the second and its sensitivity to signals coming from remote transmitters, when the spectral content of the interfering signal is within the bandwidth of the input stage filter of the receiver [1]. For the validation of the active element modeling, the input impedance of the receiver is computed, by Fourier transforming the time domain input voltage and current data of 8192 time steps. The resulting pattern of the parallel RLC combination is thus derived and compared successfully to its theoretical value (Fig. 6). Parallelizing the code, speed-ups of more than 90 were obtained on 128 processors (Fig. 7). Timing measurements for the same case are given in Fig. 8.

A second case study is shown in Fig. 9. Again, antenna 1 is considered as a transmitter, while antenna 2 is loaded by a parallel RLC block, being in receive mode. The input current waveform at antenna 1 is almost identical to the one of the previous case (only differning at some low amplitude retro-reflections). Input current and voltage waveforms for antenna 2 are given in Fig. 10. Furthermore, Fig. 11 includes three snapshots of E_x at time steps 400, 800, 1200 sampled at a $z-$ plane that includes the transmitting antenna, clearly showing the metal trunks of the vehicles and the free space propagation of the excitation pulse that is emitted from the transmitter and eventually covers the whole space, illuminating the second vehicle. Finally, for this case, speedup of more than 85 was obtained on 128 processors (Fig. 12).

V. Conclusions

A research effort to rigorously model cosite interference problems by time domain methods such as FDTD and MRTD, combined with paralellization strategies was described in this paper. Preliminary numerical results, based on the FDTD technique were derived as a basis for the physical understanding of the problem, that is fundamental for the fine-tuning of the adaptive wavelet based technique that we propose. The compatibility of our approach with SPICE type circuit simulators allows for the development of an integrated analysis tool for circuit and EM phenomena pertinent to tranceiver system performance under EMI conditions.

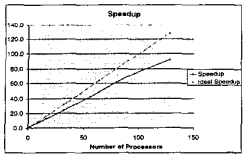

Fig. 7. Parallel speed-up curve for the geometry of Fig. 4.

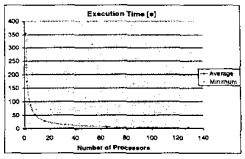

Fig. 8. Execution time with respect to processors for the geometry of Fig. 4.

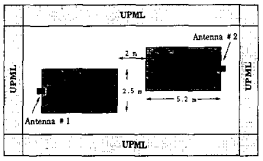

Fig. 9. Computational domain for the second cosite interference scenario ($yz-$ plane).

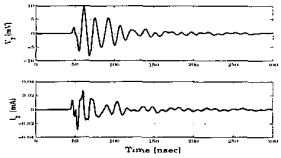

Fig. 10. Input voltage and current of antenna 2 of Fig. 9.

References

[1] J. J. Gavan, M. B. Shulman, "Effects of desensitization on Mobile Radio System Performance, Part I : Qualitative Analysis ", *IEEE Trans. Vehicular Tech., vol. VT-33, No.4, November 1994, pp. 285-290.*

[2] B. Houshmand, T. Itoh, M. Picket-May, "High-Speed Electronic with Active and Nonlinear Components", *ch. 8, in Advances in Computational Electrodynamics, the Finite Difference Time Domain Method, A. Taflove ed., Artech House, Boston, 1999.*

[3] M. Krumpholz, L.P.B. Katehi, "MRTD: New Time Domain Schemes Based on Multiresolution Analysis", *IEEE Trans. Microwave Theory and Techniques, vol.44, no.4, pp.555-561, April 1996.*

[4] E. Tentzeris, R. Robertson, A. Cangellaris, L. P. B. Katehi, "Space and Time Adaptive Gridding Using MRTD", *1997 IEEE MTT-S Digest, pp. 337-340.*

[5] C. D. Sarris, L. P. B. Katehi, "On the use of wavelets for the implementation of high order mesh refinement in time domain simulations", *Proceedings of the 30th European Microwave Conference, pp. 284-287, Paris, France, October 2000.*

[6] C. D. Sarris, L. P. B. Katehi, "Fundamental Gridding Related Dispersion Effects in Multiresolution Time Domain Schemes", *accepted for presentation in the 2001 IEEE International Microwave Symposium.*

[7] S. Grivet-Talocia, "On the Accuracy of Haar-Based Multiresolution Time Domain Schemes", *IEEE Microwave and Guided Wave Letters, vol. 10, no. 10, pp. 397-399, October 2000.*

[8] S. Gedney, "The Perfectly Matched Layer Absorbing Medium", *ch. 5 in* Advances in Computational Electrodynamics : The Finite Difference Time Domain Method, *A. Taflove, ed.*, Artech House, 1998.

[9] C. D. Sarris, L. P. B. Katehi, "Development and Application of an Efficient FDTD/MRTD Numerical Interface", *accepted for presentation in the 2001 IEEE International Microwave Symposium.*

[10] R. L. Robertson, C. D. Sarris, L. P. B. Katehi, "Analysis of Lumped Element Transistor Structures Using MRTD : The State Equation Approach", *submitted to the IEEE Microwave and Guided Wave Letters, October 2000.*

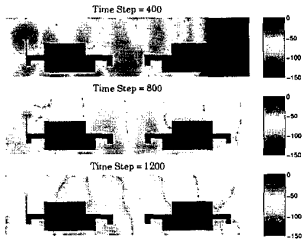

Fig. 11. E_x field pattern sampled at the $z-$plane containing antenna 1 in the geometry of Fig.9.

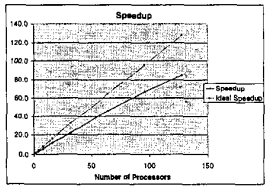

Fig. 12. Parallel speedup curve for the geometry of Fig. 9.